Naval Research Laboratory

Washington, DC 20375-5000

NRL Memorandum Report 6680

Overview of Beam Conditioning

R. F. FERNSLER, A. W. ALI, P. BORIS*, R. F. HUBBARD,
G. JOYCE AND S. P. SLINKER

Plasma Physics Division

**Science Applications International Corp.*
McLean, VA 22102

August 31, 1990

REPORT DOCUMENTATION PAGE

Form Approved
OMB No. 0704-0188

1. AGENCY USE ONLY (Leave blank)	2. REPORT DATE	3. REPORT TYPE AND DATES COVERED
	1990 August 31	Interim

4. TITLE AND SUBTITLE

Overview of Beam Conditioning

5. FUNDING NUMBERS

JO#-47-0900-0-0

ARPA Order #4395, A86

6. AUTHOR(S)

R. F. Fernsler, A. W. Ali, P. Boris,* R. F. Hubbard,
G. Joyce and S. P. Slinker

7. PERFORMING ORGANIZATION NAME(S) AND ADDRESS(ES)

Naval Research Laboratory
Washington, DC 20375-5000

8. PERFORMING ORGANIZATION REPORT NUMBER

NRL Memorandum Report 6680

9. SPONSORING/MONITORING AGENCY NAME(S) AND ADDRESS(ES)

DARPA
Arlington, VA 22209

NSWC
Silver Spring, MD 20903-5000

10. SPONSORING/MONITORING AGENCY REPORT NUMBER

11. SUPPLEMENTARY NOTES

*SAIC, McLean, VA 22102

12a. DISTRIBUTION/AVAILABILITY STATEMENT

Approved for public release; distribution unlimited.

12b. DISTRIBUTION CODE

13. ABSTRACT *(Maximum 200 words)*

This report contains five short papers summarizing theoretical studies of various techniques for conditioning relativistic electron beams. Conditioning refers to processes that either damp transverse fluctuations of the beam, or provide a head-to-tail variation in its emittance. The studies were performed in support of beam propagation experiments being conducted at several laboratories.

14. SUBJECT TERMS

relativistic electron beam
conditioning
IFR cell
wire cell
foil cell
energy-ramp cell

15. NUMBER OF PAGES

36

16. PRICE CODE

17. SECURITY CLASSIFICATION OF REPORT	18. SECURITY CLASSIFICATION OF THIS PAGE	19. SECURITY CLASSIFICATION OF ABSTRACT	20. LIMITATION OF ABSTRACT
Unclassified	Unclassified	Unclassified	SAR

CONTENTS

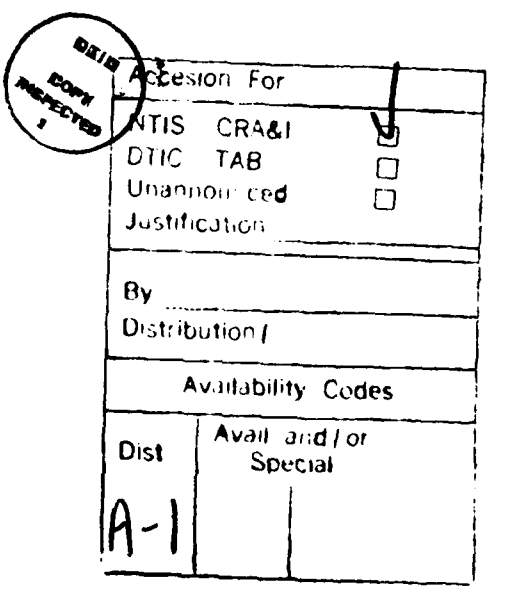

OVERVIEW OF BEAM CONDITIONING

This report contains five short papers that were presented at the Annual DARPA/SDIO/Services Charged Particle Beam Review held at the Naval Postgraduate School in Monterey, California during 18-21 September 1989. The papers describe theoretical beam conditioning studies carried out at NRL in support of propagation experiments at several laboratories.

Since these papers were written, the ATA Multi-Pulse Propagation Experiment (ATA/MPPE) has been completed, and high-current propagation has been successfully demonstrated at NRL's Super-IBEX facility. Both experiments used a passive IFR cell to taper the beam from head to tail, resulting in improved stability during subsequent propagation. The ATA experiment was plagued by substantial initial beam sweep, in part because of problems with the Fast Corrector Coil (FCC) which was designed to suppress such fluctuations. Detailed analysis of these experiments will be reported elsewhere.

A brief description of each paper and a list of authors are given below.

Beam Conditioning Techniques: This paper contains an overview of NRL research on several post-accelerator techniques used either to center a beam or to introduce a head-to-tail variation in beam emittance. The techniques discussed are passive IFR cells, vacuum and gas-filled wire cells, multi-foil cells, and energy-ramp focusing cells. Proper use of these techniques can substantially reduce the growth of the hose instability after the beam is injected into air. Both analytical modeling and simulation codes have been employed in these studies. (Fernsler, Slinker, Hubbard, Joyce)

Wire Cells I: Vacuum: Vacuum wire cells include passive devices with a simple resistive wire charged by the beam, and active devices driven by an externally applied wire current. Wires can be used both to center the beam and to taper its radius. The major disadvantages are wire fragility, beam losses to the wire, and the production of radial wings in the beam profile. Passive wire cells, moreover, do not center the beam head and generally overheat the beam body. Active (current-carrying) wire cells center the

Manuscript approved May 21, 1990.

entire beam without overheating it, provided the applied current is modest. An active cell can produce emittance tailoring if the beam radius is appropriately tapered prior to entering the wire cell. The analytical results are supported by particle simulations using the PEWW code. (Fernsler, Slinker)

Wire Cells II: Gas: An externally-driven gas-filled wire cell was examined as a possible conditioning technique for Super-IBEX. The additional pinch forces in the gas-filled cell suppress the formation of radial wings in the beam profile, but they also promote hose instability. Analytical calculations indicate that the wire current needed to damp hose will overheat the beam. In support of this prediction, SARLAC simulations showed that an externally applied wire current of 7.9 kA was insufficient to completely damp hose in a 30 kA beam, while 14.2 kA of wire current damped hose but overheated the beam. Gas-filled wire cells do provide some radius tailoring inside the cell, but it is inadequate for most propagation experiments and can be converted into emittance tailoring only at the expense of further overheating. (Slinker, Fernsler, Hubbard)

Foil Focusing for Transport and Conditioning: A thin conducting foil in a vacuum beam line focuses the beam like a thin lens. The focal length is proportional to $r_b I_A / I_b$ where r_b is the beam radius, I_b is the beam current, and $I_A = \gamma mc^3/e$ is the Alfven current. Analytic calculations of the focal length and emittance growth for various beam profiles have been confirmed by the FRIEZR particle simulation code. Some versions of FRIEZR impart a prescribed impulse to each simulation particle as it passes the foil location, while other versions solve the full electromagnetic field equations on a fine axial mesh. Both the analytical and simulation results predict that emittance growth from the anharmonic nature of foil focusing is a severe problem for beams with high I_b/I_A such as Super-IBEX. In addition, we have found that "matched" transport, in which the beam radius is constant at each foil, is not possible because the condition for matching violates the condition for stability in a periodic focusing system. Nevertheless, multi-foil transport can be useful for transport over limited distances and, in some cases, can provide emittance tailoring. (Fernsler, Hubbard, Slinker, Boris).

Beam Conditioning Options for the ATA Multi-Pulse Experiment: Stable propagation of the ATA/MPPE will require a substantial head-to-tail emittance variation. Three strategies have been considered for introducing this variation: a multi-foil cell, a differential focusing cell, and a passive IFR cell. All three have been analyzed using analytical models and axisymmetric FRIEZR simulations, and all are capable in principle of producing substantial emittance tailoring. The multi-foil cell, however, tailors the beam over too narrow a region and overheats the beam through scattering. The differential focusing cell provides considerable flexibility, but suffers from a need for fine tuning of the energy ramp. The passive IFR cell appears to produce the best tailoring, especially when operated at low gas pressures, provided the beam emittance is low at injection. (Hubbard, Slinker, Fernsler, Joyce, Ali)

BEAM CONDITIONING TECHNIQUES

R. Fernsler, S. Slinker, R. Hubbard, and G. Joyce
Beam Physics Branch, Plasma Physics Division,
Naval Research Laboratory, Washington, D.C.

INTRODUCTION

A relativistic electron beam must be conditioned to achieve stable, long-range propagation. We identify four nominal conditioning goals. First is a centering requirement relating the beam offset, y_b, to the beam radius, r_b:[1]

$$\frac{y_b}{r_b} \lesssim \begin{cases} 0.01 & \text{for high frequencies (BBU)} \\ 0.1 & \text{for low frequencies (sweep)} \end{cases} . \qquad (1)$$

Second, the normalized emittance, ε_n, should taper over 10-20 ns from a large value in the beam head to a small value in the body with a variation

$$\varepsilon_n^{(max)}/\varepsilon_n^{(min)} > 3. \qquad (2)$$

Third, the value $\varepsilon_n^{(min)}$ in the body should be small to maintain a tight pinch. And fourth, the beam should exit the final conditioning cell well matched for propagation into air.

In this paper we briefly summarize theoretical predictions for several conditioning techniques. Papers 2-5 describe the results in more detail.

We begin with four observations. First, the emittance prior to conditioning should be small: $\varepsilon_n^{(inj)} < 0.5\ \varepsilon_n^{(min)}$. Second, ε_n, rather than r_b alone, should be tailored to detune the hose instability (because past the pinch point, $\lambda_\beta \propto \varepsilon_n/I_{eff}$). Third, using foil scattering to tailor ε_n works only if r_b is flared. And fourth, two cells generally work best using the first cell to flare r_b and the second cell to heat and center the beam; a thick exit foil is then unnecessary and undesirable.

PASSIVE IFR CELL

A passive IFR cell consists of a tube filled with low-density (P < 1 Torr), un-ionized gas. The beam ionizes the gas and electrostatically ejects

*Work supported by the Defense Advanced Research Projects Agency, ARPA Order No. 4395, Amendment 80, monitored by the Naval Surface Warfare Center

the plasma electrons, leaving the ions to pinch the beam. The developing ion pinch flares r_b and partially centers the beam. The principal concerns are ion motion, magnetic trapping of plasma electrons at high beam current, I_b, and gas heating and recovery. Our studies indicate that IFR cells flare r_b well, even at high I_b, provided P ~ 10 mTorr and $\varepsilon_n^{(inj)} < 0.5\ \varepsilon_n^{(min)}$; see the example below. A thick exit foil or later heating cell would convert the radius flare into emittance tailoring. IFR cells additionally damp high-frequency offsets y_b in the beam body.

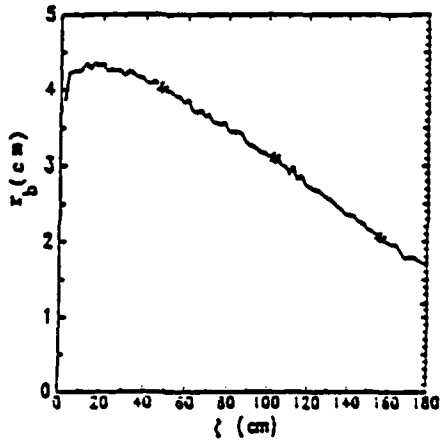

Fig. 1. IFR Cell (20 mTorr air): I_b = 50 kA, γ = 8, z = 30 cm.

WIRE CELLS

Several different wire conditioning schemes have been studied. Passive vacuum wire cells, consisting of a thin resistive wire in an evacuated pipe, flare r_b, center the body (though not the head), but inverse tailor the beam and overheat it by ~ $I_b/I_{eff} > 1$, where I_{eff} is the effective current in air. Adding a thick exit foil to tailor ε_n overheats the beam more. By contrast, an active vacuum wire cell, consisting of a highly conducting wire with external current, I_{ext}, centers the entire beam without overheating, provided $I_{ext} \leq I_{eff}/2$. Moreover, the active cell can convert a flare in r_b (from, say, a preceding IFR cell) into tailoring of ε_n. Vacuum wire cells suffer, however, from losses to the wire and from electron profiles with broad radial wings about a sharply peaked center. A small wire reduces the losses but is fragile and, at high I_b, must be replaced after each shot. See Ref. 3 for further discussion of vacuum wire cells.

An active gas-filled wire cell consists of a highly conducting wire with

I_{ext} but in gas. The self-pinch force from the beam improves beam profile but allows for hose instability, as illustrated below. I_{ext} must be large to suppress hose but small to avoid beam overheating. The best compromise is to damp hose but overheat the beam by a factor of 2 or less, depending upon I_b and the pulse length. Note that a gas cell inverse tailors ε_n, even with a γ-ramp, unless r_b is flared at injection. See Ref. 4 for further discussion.

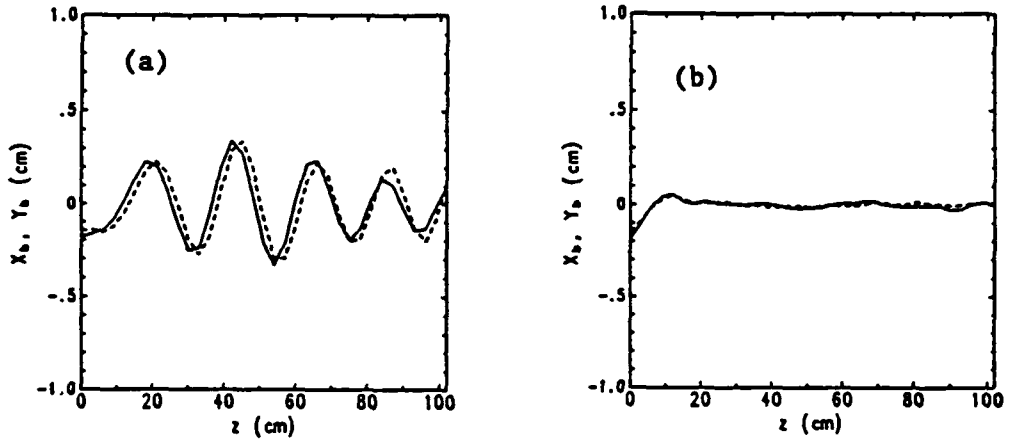

Fig. 2. Gas Wire Cell showing: (a) hose growth for I_{ext} = 7.9 kA, and (b) hose damping for I_{ext} = 14 kA. Here I_b = 30 kA, γ = 10, and ζ = 1080 cm.

FOIL CELLS

Transverse conducting foils act in vacuum like thin lenses with a focal length proportional to $r_b\gamma/I_b$. A ζ-variation in beam impedance, γ/I_b, can therefore be used to flare r_b. Because foils are imperfect lenses, however, they quadradically increase ε_n by an amount proportional to $(r_bI_b)^2$. Foil scattering, if present, further increases ε_n quadradically by an amount proportional to r_b^2 times the foil thickness. Using foils to flare r_b, and ultimately tailor ε_n, is thus practical only for $I_b \ll I_A \approx 17\gamma$ kA. Moreover, tailoring occurs only where γ/I_b varies. See Ref. 5 for details.

ENERGY-RAMP FOCUSING CELL

An energy-ramp focusing cell consists of a solenoidal lens, a thick scattering foil, and a prescribed variation in γ with ζ. Because the focal length of a solenoidal lens varies as γ^2, a 20% variation in γ can be converted into a large radius flare downstream of the lens. Passing the flared beam through a thick scattering foil (after allowing for foil focusing) produces emittance tailoring. This technique requires a highly

reproducible energy variation, $\gamma(\zeta)$, and a small energy spread, $\Delta\gamma/\gamma \ll 1$, at any given ζ. The latter condition necessitates $I_b \ll I_A$. Moreover, overall performance is sensitive to foil location, and the solenoidal field errors must be small. See Ref. 2 for discussion.

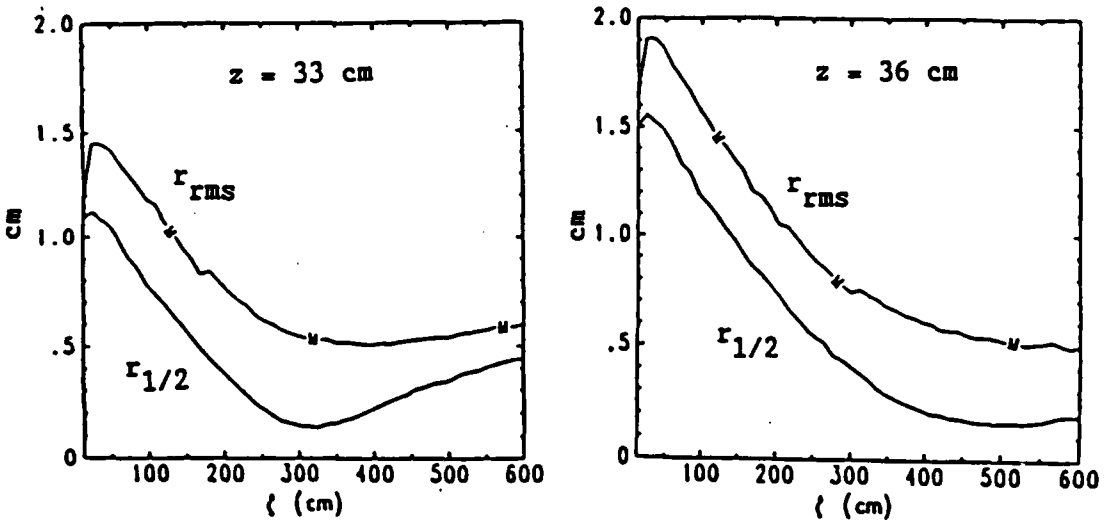

Fig. 5. Energy-Ramp Tailoring Cell: 6 kA, 8-10 Mev variation over 10 ns, perfect solenoidal lens with a nominal focal length of 30 cm.

CONCLUSION

IFR cells appear to be the best candidate for radius-flaring, in terms of emittance degradation and ease of control. The best technique for centering is the active wire cell, gas or vacuum, which provides control and rapid phase-mix centering. An attractive variation is a filamentary gas discharge which would eliminate wire losses and wire replacement (at low rep-rates).

REFERENCES

1. R.F. Hubbard, et al., "Sensitivity of Hose Instability to Frequency of Initial Perturbations", these proceedings.
2. R.F. Hubbard, et al., "Beam Conditioning Options for the ATA Multi-Pulse Experiment", these proceedings.
3. R.F. Fernsler, et al., "Wire Cells I: Vacuum", these proceedings.
4. S.P. Slinker, et al., "Wire Cells II: Gas", these proceedings.
5. R.F. Fernsler, et al., "Foil Focusing for Transport and Conditioning", these proceedings.

WIRE CELLS I: VACUUM*

R. Fernsler, S. Slinker
Beam Physics Branch, Plasma Physics Division
Naval Research Laboratory, Washington, D.C.
P. Boris
SAIC, McLean, VA

INTRODUCTION

In this paper we summarize our present theoretical understanding of active and passive vacuum wire cells as devices for centering or tailoring relativistic electron beams. The analytic theory is reviewed first, followed by numerical simulations. Gas-filled wire cells are considered separately in the companion paper, "Wire Cells II: Gas."

THEORY

In this section we present results from analytic calculations. We begin with a brief description of passive and active wire cells.

A passive vacuum wire cell consists of a thin resistive wire centered in an evacuated pipe with conducting end plates.[1] The beam induces a charge λ_w and current I_w on the wire. The wire resistance R_w resistively damps I_w in a time L_w/R_w, where L_w is the wire inductance. As a consequence, an electrostatic pinch force (from λ_w) develops with time.

An active vacuum wire cell uses a highly conducting wire with an external current.[2] Because $R_w = 0$, the attractive and repulsive forces from the induced wire charge and current nearly cancel, leaving the magnetic force from the external current, I_{ext}, to pinch and center the beam.

Away from the end plates and to order γ^{-2}, the only force on the beam electrons is the wire force, $F_w = -2T_w/r$ where $T_w \equiv e(I_w/c - \lambda_w)$. The large spread in electron oscillation frequency, $\omega_\beta \propto 1/r$, causes rapid phase-mix damping so that the beam quickly centers and equilibrates about the wire.

Inside the wire cell, the average equilibrium beam temperature is given, independent of injection conditions, by

$$T = -\frac{1}{2}\int_0^\infty dr \, \frac{2\pi r J_b}{I_b} \, r F_w(r) = T_w$$

*Work supported by the Defense Advanced Research Projects Agency, ARPA Order No. 4395, Amendment 80, monitored by the Naval Surface Warfare Center.

to order $a_w^2/a_b^2 \ll 1$. Here a_w is the wire radius, a_b is the beam radius, J_b is the beam current density, and I_b is the beam current. By contrast, the equilibrium temperature of a self-pinched, self-similar beam in air is given by $T_B = eI_{eff}/2c$, where $I_{eff} < I_b$ is the effective current. An active wire cell thus does not overheat the beam ($T_w \leq T_B$) provided

$$I_{ext} \leq I_{eff}/2.$$

However, in a passive wire cell, $I_w \to 0$ while $\lambda_w \to \sim -I_b/2c$. Hence, a passive cell overheats the beam by a factor

$$T_w/T_B \simeq I_b/I_{eff} > 1.$$

Adding a thick exit foil overheats the beam further.

The 1/r dependence of F_w produces beam profiles strongly peaked about the wire. For example, for an isothermal beam about a hollow wire,

$$J_b(r) \to J_b(0)\ (a_w/r)^{2x},$$

where

$$x = H(a_w-r)/(1-a_w^2/a_b^2).$$

Here H is the Heaviside step function, and $a_b^2 \equiv I_b/\pi J_b(0)$. For $r > a_w$ and $a_b \gg a_w$, $x \simeq 1$. For a beam that is injected cold and nearly flat-topped, the equilibrium beam current density still peaks about r = 0 but falls off more gradually with a sharp cut-off at the initial edge radius, $a_i \gg a_w$:

$$J_b(r) \to (I_b/\pi a_i^2)\ [(a_i-r)/(r+a_w)]\ H(a_i-r).$$

The minimum beam emittance can estimated by showing that a cold beam at injection contracts according to

$$\langle r^n \rangle \simeq (n+1)^{-1/2} \langle r_i^n \rangle,$$

where $\langle r_i^n \rangle$ is the nth radial moment at injection. Combining this result with the result for $T = T_w$ yields a minimum normalized emittance given by

$$\varepsilon_n^{(min)} \simeq \gamma R_i \left[(I_w - c\lambda_w)/I_A\right]^{1/2},$$

where R_i is the rms radius at injection and $I_A \simeq 17\gamma$ kA is the Alfven current. The passive wire cell thus inverse tailors ε_n. On the other hand, the active wire cell tailors ε_n, for constant I_{ext}, only if R_i flares in the head (or γ falls with ζ). Note that a γ-ramp produces inverse tailoring for both cells and is therefore usually detrimental.

Losses to the walls and wire are a major concern for solid beams. By considering the turning radii of the electron orbits, we have concluded that the wall losses are small provided the beam temperature at injection is small, $T_i < T_w/2$, and the wall radius large, $b > 2\ R_i$. Losses to the wire should be small provided $T_i \geq T_w/5$ and $a_w \leq 0.01\ R_i$; here, finite T_i imparts angular momentum to the beam electrons, causing most to miss the wire (much as occurs for hollow, rotating beams such as RADLAC). A related concern is wire durability which typically is poor at high beam currents and long pulses; the wire must then be replaced after each shot.

SIMULATIONS

We have used the PEWW code to simulate both the passive and active wire cells. This code combines a fully relativistic particle pusher (courtesy of G. Joyce) and an ultrarelativistic circuit equation to compute I_w and λ_w. End-plate effects are not included in the simulations presented.

A passive wire cell of length $L = 1$ m and radius $b = 14.8$ cm, with a wire resistance $R_w = 1\ \Omega$/cm and radius $a_w = 0.05$ cm, is simulated below. The beam current I_b rose to 10 kA in 5 ns with $\gamma = 10$, half-radius $R_{1/2} = 1$ cm, and $\varepsilon_n = 2.3$ rad-cm. The beam was injected off-axis at $\bar{x} = -0.5$ cm. Plotted at cell exit are $R_{1/2}$ and R, ε_n, and the centroid $\bar{x}$. Observe that the cell flares R, inverse tailors ε_n, and centers the beam body but not the head. The cell overheats the beam by ~ 30%, relative to the Bennett temperature in air. Adding a thick exit foil to tailor ε_n would overheat the beam further.

We next show a simulation of an active cell with $L = 1$ m, $b = 20$ cm, $R_w = 0$, $a_w = 0.08$ cm, and $I_{ext} = 5$ kA. I_b rose to 20 kA in 12 ns with $\gamma = 10$ and a matching current $I_m = 1.7$ kA. The beam was injected off-axis at $\bar{x} = -0.5$ cm with R flared as shown. The beam at exit is well centered and emittance tailored.

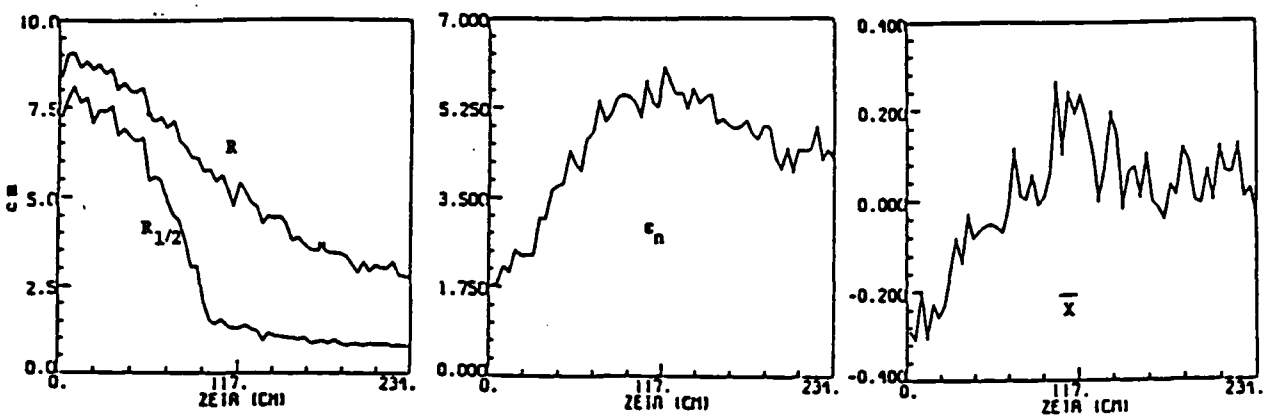

Fig. 1. A passive vacuum wire cell.

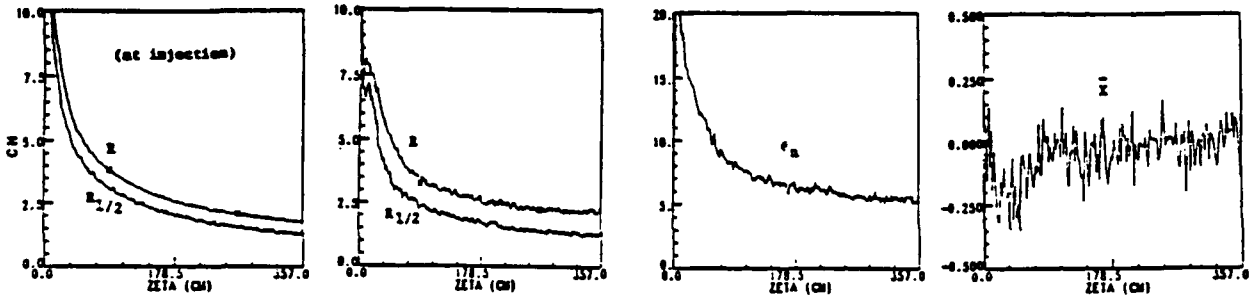

Fig. 2. An active vacuum wire cell (flared beam at injection).

CONCLUSION

A passive vacuum wire cell flares the radius, centers the body but not head, and overheats the body. The overheating becomes substantial at beam currents above 10 kA. An active cell centers the entire beam without overheating, and tailors the emittance if the beam is flared at injection.

REFERENCES:

1. D.S. Prono, et al., IEEE Trans. Nuc. Sci. NS-30, 2510 (1983).
2. J.R. Freeman, et al., Proc. 1988 DARPA Review 1, 147 (1989).

WIRE CELLS II: GAS*

S. Slinker, R.F. Fernsler and R.F. Hubbard
Plasma Physics Division
Naval Research Laboratory

Introduction. An externally-driven, current-carrying wire immersed in a gas (normally ambient air) has shown promise as a technique for beam conditioning. Experiments on IBEX and RADLAC at SANDIA(1) verify the excellent centering and transport properties of these cells. Theoretical modeling and numerical simulation of gas-filled wire cells has been performed by both SANDIA(2) and MRC(3). This paper investigates the feasibility of using gas-filled wire cells on the SUPERIBEX experiment.

Advantages of gas-filled wire cells. 1). These cells have strong centering and damping properties. The force, going inversely with r, is very anharmonic giving good phase-mix damping. The length of the cell need be only a few betatron wavelengths: $L \sim$ a few $2\pi r_b(17\gamma/I_{eff})^{1/2}$. By integrating the frozen field approximation to Maxwell's equations, one can show that the total current in the wire I_w, including the return current induced by the presence of the beam, is given approximately by $I_w \sim I_d - I_{net}/2$ where I_d is the current driven in the wire before the beam enters and I_{net} is net current the beam would have if the wire weren't there. This assumes the inductance in the external circuit is small compared to the cell. The minimum amount of driven current I_d for the cell to work is that which allows $I_w > 0$; that is, $I_d > I_{net}/2$ is required. If this requirement is not met, the wire will repulse the beam.

*Work supported by the Defense Advanced Research Projects Agency, ARPA Order No. 4395, Amendment No. 80, monitored by the Naval Surface Warfare Center.

Because of the plasma currents in the gas, the hose instability may occur in the cell. To damp hose the driven current I_d must exceed the requirement mentioned above. Certainly, if the force from I_w exceeds the repulsive force from the plasma current driven by the beam in the gas, then hose perturbations cannot grow. This requirement can be estimated by

$$I_w \sim -\pi r_b^2 \int_{r_w}^{\infty} dr \frac{2\pi r J_b}{I_b} \sigma E_z \equiv -gI_p ,$$

where g is a geometric factor which is 1/3 for Bennett beams and 1 for flattop beams with self-similar plasma currents. With the relationship between I_w and I_d given above, this translates into an upper bound for the minimum driven current needed to completely damp hose: $I_d \sim gI_b + (.5-g)I_{net}$. For a 30 kA Bennett beam with a net current of 10 kA the minimum required driven current is between 5 kA and 12 kA, while a flattop may need up to 25 kA.

2). The gas-filled wire cell can generate some radius flaring which can be transformed to emittance tailoring by scattering in an exit foil. This results from variation of the effective current due to the rise in beam current and also from gas scattering in a beam with energy variation.

3). Because part of the pinch force is beam-generated, a better radial profile (smaller wings) is given to the beam in contrast to an externally-driven wire cell in vacuum.

4). The gas-filled cell is easier to implement experimentally than a vacuum cell.

<u>Disadvantages of gas-filled wire cells.</u> 1). The cell tends to heat the beam too much. The effective current in the cell is given by $I_{eff} = 2I_d + I^u_{eff}$ where I^u_{eff} is the effective current of the beam in the presence of the wire without any driven current present. It is a fraction of the effective current in open air. For the 30 kA beams simulated below the effective current in open air was ~ 10 kA while

I^u_{eff} was ~ 4 kA. For the beam to be matched into air the effective current in the cell should match that in the open air. Clearly this requirement is incompatible with the requirements on I_d needed for centering and damping, so some mismatch has to be tolerated and the beam will expand at exit. Fortunately the equilibrium radius depends on the square root of the effective current. Note that using a thick exit foil to emittance tailor will enhance the mismatch. Also using a large inductance in the external circuit to clamp the driven current, while lessening the minimum stablizing requirements, will overheat the beam.

2). Using the cell with solid beams (SUPERIBEX) will result in wire loss of beam electrons. This may not be a problem if there is "current to burn". In any case a possible solution may be to drive the external current through a filamentory discharge. This is also a possible solution for multi-pulse applications provided channel expansion is tolerable.

3). The radius tailoring achievable by this cell (probably not much better than 2:1) is not adequate for most applications. Consequently, this cell must be used with other conditioning means. The best configuration may be to emittance tailor the beam before it enters the gas-filled wire cell and use this cell mainly to center.

Simulation model. Propagation in the gas-filled wire cell was modeled with SARLAC. A large, but finite, conductivity σ_d was put in a narrow region, $r_w \sim .08$ cm, at the axis. An external current density, $J_d = I_d/\pi r_w^2$, is used as a source term in the field solver. For these runs the injected beam was Bennett with a small amount of tailoring. There was a γ ramp from 4 to 10 over the 13 ns rise of the beam. The peak beam current was 30 kA. The timestep had to be on the order of .125 cm in order to resolve motion near the wire.

Simulation results. With a wire radius of 0.079 cm and a solid SUPERIBEX beam of 30 kA, about 10 kA was lost in a 100 cm cell. Though this is an overestimate of wire loss, since any electron which hit the wire was discarded, it was decided to ignore the wire loss problem in

the rest of the simulations and assume they pass through without loss or deviation. In particular, wire losses can be minimized by using a fine wire or a discharge.

The main results consist of a scan of cell currents. Three values of I_d were tried: 3.16, 7.9 and 14.2 kA. The beam current rose to 30 kA over 13.3 ns. The nominal beam radius was 1 cm. There was a 2.5 to 1 emittance tailoring over 13.3 ns due to radius variation in the injected beam. The discharge radius was 0.079 cm and the cell length was 100 cm. The beam was injected with a low frequency hose perturbation of at most 0.28 cm off the discharge center.

The results are summarized in the following table along with code verifications of some of the simple scaling formulas.

CODE RESULTS

CASE	I_w @ 14ns	I_{eff} @ head	I_{eff} @ 14ns	I_{net} @ 14ns	$R_{1/2}$ @ exit	R_{rms} @ exit	ε_n @ exit
$I_d=0, \sigma_d=0$		0	9.7	10.2			
$I_d=0$	-5.6	0	3.9	8.8			
$I_d=3.16$	-1.9	4.2	10.2	12	2.4	3.6	11
$I_d=7.9$	2.8	16.2	19.8	16.6	1.2	2.7	8.7
$I_d=14.2$	8.8	25.2	32.3	23.8	1.1	2.6	10.9

For the 14 ns slice at entrance: $R_{1/2} = 1$, $R_{rms} = 2.9$ and $\varepsilon_n = 5.4$.

Formula # 1:

$$I_w = I_d - I^*_{net}/2$$

Code gives: I_d	I^*_{net}
0	11.2
3.16	10.2
7.9	10.2
14.2	10.8

Formula # 2:

$$I_{eff} = 2\, I_d + I^u_{eff}$$

Code gives: I_d	I^u_{eff}
0	3.9
3.16	3.9
7.9	4.0
14.2	3.9

Formula # 3:

$$\varepsilon_n = \gamma R_{rms} (I^*_{eff}/17\gamma)^{1/2}$$

Code gives: I_d	I_{eff}	I^*_{eff}
3.16	10.2	15.9
7.9	19.8	17.7
14.2	32.3	29.7

Formula # 4: the minimum I_d for hose stability satisfies

$I_{net}/2 - 5 < I_d^m < 11.7$ for a Bennett

Code gives:

$7.9 < I_d^m < 14.2$

For both the 7.9 and 14.2 values of the external current, the slice at 14 ns centered and damped at once, reaching a value about an order of magnitude down by the end of the cell, while the displacement grew for I_d = 3.16. A slice at 36 ns has its displacement grow to about 0.5 cm off axis before damping when I_d = 7.9. For 14.2 kA all slices damped immediately in the cell. Therefore, the minimum amount of I_d needed to completely damp hose growth was between 7.9 and 14.2 kA.

The beam exiting the 7.9 kA cell had an emittance fairly well matched at the 14 ns point to that in open air (without an exit foil). It was then propagated for 2 m and its stability was compared to that of a beam with the same parameters as that entering the gas cell but with a higher temperature in order to match open air. After a meter of propagation the gas-cell-conditioned beam showed much smaller hose growth, but the differences were not great at the 2 m propagation point. The beam radii at 2 m were comparable. This indicates that the major effect of the cell was to dampen the displacements at the expense of tailoring. Obviously a better tune, along with an exit foil, is needed.

Conclusions. The gas-filled wire cell shows promise as a centering and damping device for SUPERIBEX. The major disadvantages are beam overheat and current loss if a wire is used. Tailoring is not sufficient and so the cell must be used in conjunction with some other tailoring device.

References.

(1). C. Frost, these proceedings.
(2). J. Poukey, J. Freeman, private communication.
(3). D. Welch, these proceedings.

FOIL FOCUSING FOR TRANSPORT AND CONDITIONING*

R. Fernsler, R. Hubbard, S. Slinker
Naval Research Laboratory, Washington, D.C.
P. Boris,
SAIC, McLean, VA.

INTRODUCTION

Adler[1] and Humphries[2] have proposed foil focusing as a means of transporting electron beams, while Fawley[3] has proposed foil focusing for conditioning. In this paper we address various issues relating to the use of foils for transporting and conditioning ultrarelativistic beams.

FOCAL LENGTH

An isolated foil may be treated as a thin lens of focal length f_ℓ provided $f_\ell \gg b$ and $b\,\partial/\partial\zeta \ll 1$, where the pipe radius b characterizes the axial range of the foil fields and $\zeta = ct - z$ measures distance behind the beam head. We have extended the analysis of Adler to compute f_ℓ for four beam profiles: flat-topped, Gaussian, parabolic, and Bessel. Plots of f_ℓ in units of $RI_A/(1-f_c)I_b$ versus r/R are shown below for three values of b/R; here R is the rms beam radius, $I_A = 17\gamma$ kA is the Alfven current, and f_c (= 0 in vacuum) is a plasma charge-neutralization fraction. We conclude from these plots that: (i) f_ℓ is relatively insensitive to beam profile; (ii) the

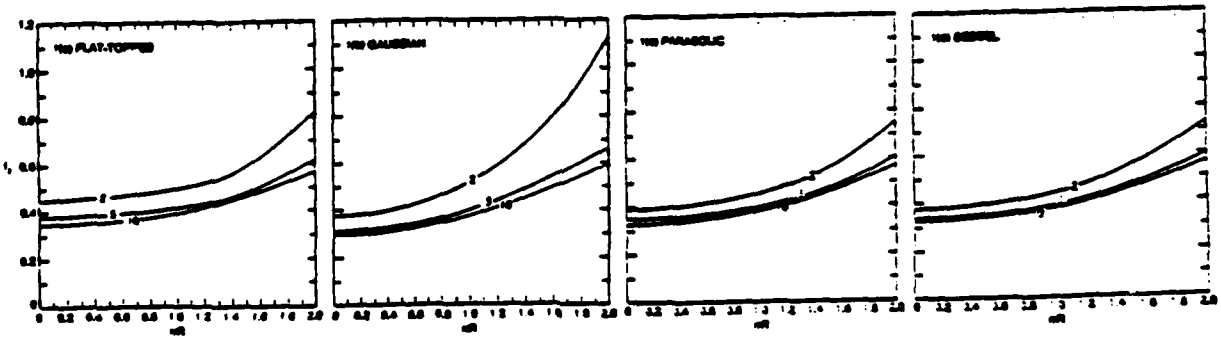

Fig. 1. Focal length f_ℓ in units of $RI_A/(1-f_c)I_b$ for b/R = 2, 5, 10.

* Work supported by the Defense Advanced Research Projects Agency ARPA Order No. 4395, Amendment No. 80, monitored by the Naval Surface Warfare Center.

paraxial treatment ($f_\ell \gg b$) is valid only if $(1-f_c)I_b/I_A \ll 0.2$; and (iii), foils are imperfect lenses with $\partial f_\ell/\partial r \neq 0$.

EMITTANCE GROWTH

We have found that a thin lens alters the normalized beam emittance ε by

$$\delta\varepsilon^2 = \varepsilon_{fo}^2 + \varepsilon_{f1}^2$$

where

$$\varepsilon_{fo}^2 = \gamma^2 \left[R^2 \langle (r/f_\ell)^2 \rangle - \langle r^2/f_\ell \rangle^2\right]$$

and

$$\varepsilon_{f1}^2 = 2\gamma^2 \left[R^2 \langle u_r r/cf_\ell \rangle - \langle r^2/f_\ell \rangle \langle u_r r/c \rangle\right].$$

Here $u_r(r)$ is the radial fluid velocity at r. Some general properties are: (i) $\delta\varepsilon = 0$ for a perfect lens (constant f_ℓ); (ii) $\delta\varepsilon$ is independent of the thermal velocity, $\delta\underset{\sim}{v}_\perp = \underset{\sim}{v}_\perp - u_r\hat{r}$; and (iii), $\varepsilon_{f1} = 0$ if the beam expands self-similarly ($u_r \propto r$). Hence, unless the beam profile changes radically, the emittance increases quadradically by ε_{fo}^2.

Using the previous results for f_ℓ, we find that for foils

$$\varepsilon_{fo} = g_3 \, R \, (1-f_c) I_b/17 \text{ kA}$$

where $g_3 \approx 0.1$ for flat-topped profiles, $g_3 \approx 0.2$ for parabolic and Bessel profiles, and $g_3 \approx 0.5$ for Gaussian profiles. The use[3] of flat-topped profiles may thus considerably underestimate the emittance increase produced by anharmonic foil focusing. Observe that ε_{fo}, like the emittance increase from foil scattering, is independent of beam energy γ. A foil thus tailors ε only if R (or I_b) varies with ζ.

MULTI-FOIL TRANSPORT:

Interactions between adjacent foils become important at foil spacings $d \lesssim b$. The preceding theory of foil focusing can, however, be readily adapted provided the focal length within each foil cell satisfies $f_\ell \gg d$. This condition becomes the new paraxial condition and allows the foil cells to be treated as separate thin lenses.

Simple ray optics[4] shows that a beam passing through a series of lenses at fixed spacing d and constant f_ℓ is stable provided $d < 4f_\ell$. For a harmonic lens but with $f_\ell \propto R$, we find that stability requires $d < 2f_\ell$, twice as restrictive as for constant f_ℓ. At very large R, saturation occurs. We have also derived a general "matching condition" for a beam of given emittance ε:

$$d = 2f_\ell \{1 + [1 - (\gamma R_{min}^2/f_\ell \varepsilon)^2]^{1/2}\} > 2f_\ell,$$

where R_{min} is the (minimum) radius between foils. Because this condition violates the stability criterion, we conclude that a matched, stable beam is not possible with foils - i.e., the beam must vary from one foil cell to another. Moreover, emittance growth from anharmonic focusing or foil scattering eventually causes the radius to grow linearly with foil number n.

FRIEZR SIMULATIONS

We have run two types of FRIEZR simulations: those that explicitly compute the foil fields, and those that use the thin-lens formalism. The former can treat a broader class of problems, but it requires small spatial and temporal steps to resolve the foil fields. The full code typically agrees with the theoretical calculations for the focal length and emittance growth to within 20%. Moreover, simulations of multi-foil transport are consistent with the analytical predictions for stability and radius growth, even at high I_b/I_A where the paraxial approximation and the analysis fail.

The use of foils for conditioning was examined using the thin-lens approximation in FRIEZR. Shown below are typical results for ATA using 2-mil carbon foils at z = 0, 39, 60 cm and 30-mil at z = 78 cm in an evacuated tank of radius 7 cm. The beam parameters were $\gamma = 21$, $I_b = 6$ kA with a 10 ns rise, R = 1 cm, and $\varepsilon = 0.46$ rad-cm. Although R and ε are well tailored at exit, ε is higher than desired in the tail. Such overheating worsens at higher I_b/I_A.

CONCLUSIONS

Our analysis and simulations indicate that foil transport and conditioning work best at low I_b/I_A and short distances. At high I_b/I_A, emittance growth from scattering or anharmonic focusing becomes excessive,

and this growth accelerates as the beam expands. For transport, we have found that the foil spacing must be kept small to prevent unstable growth.

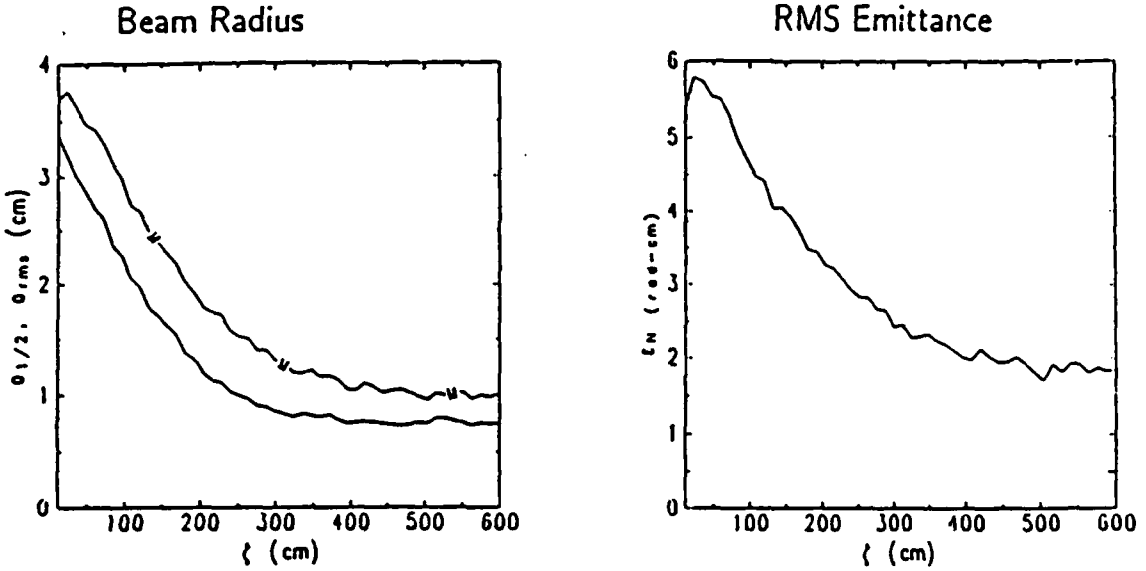

Fig. 2. ATA Multi-Foil Tailoring Cell (z = 78 cm).

REFERENCES

1. R. J. Adler, Part. Accel. 12, 39 (1982).
2. S. Humphries, Jr., Part. Accel. 13, 247 (1983).
3. W. M. Fawley, private communication.
4. S. Humphries, Jr., Principles of Charged Particle Acceleration, John Wiley & Sons, New York, 1986, p. 182. The condition given by Humphries, $d \leq 4f_\ell$, pertains only to exponential growth. Linear (unstable) growth occurs at $d = 4f_\ell$. In general, $d < 4f_\ell$ is required for stability.

BEAM CONDITIONING OPTIONS FOR THE ATA MULTI-PULSE EXPERIMENT*

R. F. Hubbard, S. P. Slinker, R. F. Fernsler, G. Joyce and A. W. Ali
Plasma Physics Division, Naval Research Laboratory, Washington, DC 20375

I. INTRODUCTION

The ATA Multi-Pulse Propagation Experiment (MPPE) will be the first serious attempt to study beam stability, tracking and range extension for a WIPS-mode pulse train. The accelerator is expected to produce 5 beam pulses separated by 1.25 msec with peak current I_0 = 6-8 kA, radius a_0 = 0.5 cm and a nominal energy of 10 MeV. However, it is expected that the beam will be disrupted by the resistive hose instability unless a substantial head-to-tail variation in beam emittance is introduced.[1] This paper examines three emittance tailoring techniques which are currently being considered for ATA/MPPE: a multi-foil cell, a classical (passive) IFR cell and a differential focusing or energy variation system. All three techniques introduce a beam radius variation $a_b(\zeta)$ where $\zeta = ct - z$ is the distance from the beam head; the beam is then passed through a final scattering foil which converts much of this variation to a variation $\varepsilon_n(\zeta)$ in the normalized emittance. Our studies have primarily been performed using the FRIEZR axisymmetric simulation code.

II. MULTI-FOIL TAILORING CELLS

Description of technique: When a relativistic beam passes through a thin conducting foil, the radial electric field is shorted out, and the beam experiences a focusing force similar to that produced by a solenoidal magnetic lens.[2,3] The focal length f_L scales with $a_b\gamma/I_b$. Fawley[4] has proposed using three thin foils positioned so that the beam body ($I_b = I_0$) is focused to a small radius while the lower current beam head expands to a larger radius. Since γ is nearly constant in ATA, the radius profile $a_b(\zeta)$ arises from the rise in beam current $I_b(\zeta)$ in the beam head.

Modifications to FRIEZR simulation code: The FRIEZR code has been upgraded to include foil focusing, scattering, and solenoidal lenses. Foils and lenses may be located anywhere in the beamline. Foil focusing is treated using a thin lens approximation:[2,3] each beam electron is given an inward impulse with a focal length whose variation with r is shown in Fig. 1 of Ref. 3, assuming a Bessel beam profile. Foil scattering is treated by imparting an appropriate random kick to each simulation particle as it passes through the

foil. Solenoidal lenses are treated by specifying a focal length f_L at the lens location and adding an impulse $\delta p_x/p_z = -x/f_L$ and $\delta p_y/p_z = -y/f_L$.

Simulation results for multi-foil cell: A series of simulations were performed for a 6 kA, 10 MeV beam with an injection beam radius $a_b(0) = 0.8$ cm, wall radius b = 7 cm, beam rise length $\zeta_r = 360$ cm, initial normalized emittance $\varepsilon_n(0) = 0.5$ rad-cm and an upstream lens placed so that $da_b/dz = 0.03$ at the first foil. Carbon foils 2 mils thick were placed at z = 0, 39, and 50 cm with a thicker 30 mil foil at z = 78 cm. (Fawley suggested similar foil locations for a shorter three-foil cell). Figure 1 plots the half-current and rms beam radii (lower and upper curves, respectively) as functions of ζ at the final foil. The desired beam taper is produced with $a_{1/2}$ varying by a factor of 4.5. The corresponding emittance taper is shown in Fig. 2. At ζ = 600 cm, ε_n is almost a factor of four above its injection value. This is due primarily to scattering, but a portion arises from weak variations in focal length length contained in Eq. (1). The latter effect is proportional to $a_b \nu_b/\gamma$ and can result in huge emittance increases for high ν/γ beams such as SuperIBEX.

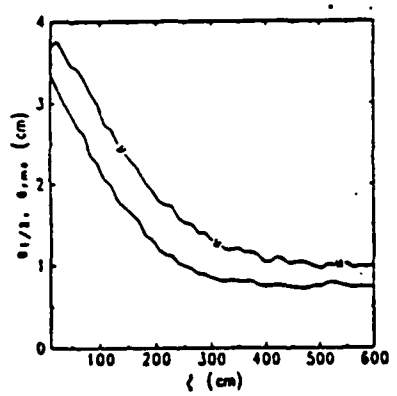

Fig 1. Beam $a_{1/2}$ and a_{rms} vs ζ at end of 78 cm long 2-2-2-30 mil carbon multi-foil cell.

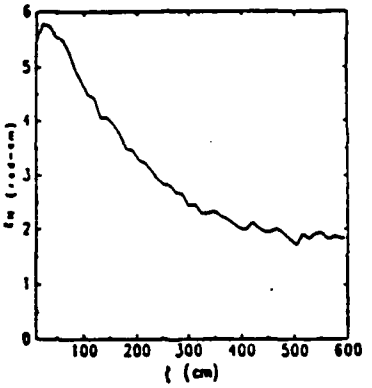

Fig 2. Emittance vs ζ for the cell used in Fig. 1. Location is just after final foil.

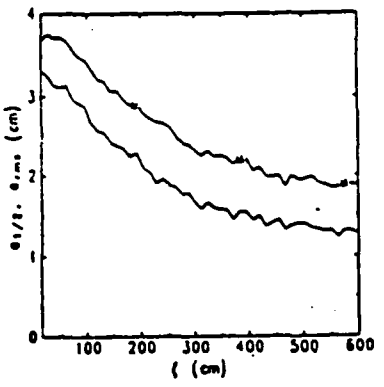

Fig 3. Beam $a_{1/2}$ and a_{rms} vs ζ at end of 78 cm long 5-5-5-30 mil carbon multi-foil cell.

When foil scattering is eliminated, the minimum half-current radius drops from 0.7 cm to 0.4 cm. However, even 2-mil foils are unlikely to survive multi-pulse ATA operation. When the first three foils are 5-mil, a_b rises to an unacceptable 1.3 cm, as shown in Fig. 3. Thus, foil scattering may severely limit the usefulness of this technique for ATA. Also, the relatively sharp radius taper in Fig. 1 is not favorable for hose stabilization.

III. PASSIVE IFR TAILORING CELL

Description of technique: Passive or classical IFR cells have been extensively used on ATA in the past to taper the beam. The beam is passed through a low pressure gas, producing a plasma column whose density, $n_i(\zeta)$, increases during the pulse. Provided $n_i < n_b$, the radial electric field produced by the beam density, n_b, expels plasma electrons, leaving behind an ion column which electrostatically pinches the beam. FRIEZR has been extensively used in the past to model such conditioning cells.[5]

IFR cells in multi-pulse operation: Although passive IFR cells have not been operated in a multi-pulse machine, we believe the beam will be tailored in the same manner as in single pulse operation. The dominant atomic physics process between pulses is expected to be charge exchange between fast ions and ambient neutral gas atoms or molecules. Hole boring should be insignificant because the collisional mean free paths are large at these gas densities. By the time the next pulse arrives, the plasma density is expected to be much to low to influence the beam. We believe that IFR cells on ATA have performed well, especially considering the inverse tailoring apparently produced by laser-ion guiding in the accelerator.

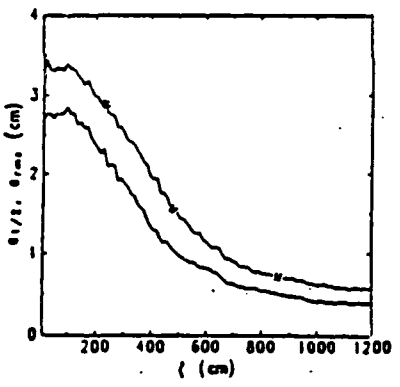

Fig 4. Beam $a_{1/2}$ and a_{rms} vs ζ at end of a 5 mtorr passive IFR cell.

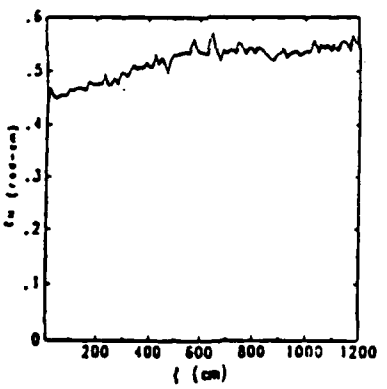

Fig 5. Beam emittance vs ζ just before final scattering foil for the IFR cell in Fig.4.

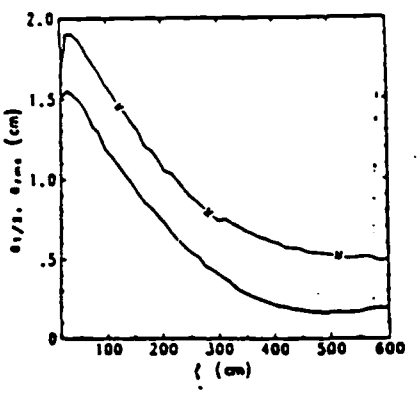

Fig. 6. Beam $a_{1/2}$ and a_{rms} for a differential focusing cell with a 20% energy variation.

Simulation results for a passive IFR cell: Although most experiments and simulations in the past have utilized IFR cell pressures of 20 mtorr or higher, lower pressures may be more effective if the beam emittance is not too large. Figure 4 plots $a_{1/2}(\zeta)$ and $a_{rms}(\zeta)$ at z = 90 cm for a beam similar to that described in the previous section. The gas was assumed to be air at 5

mtorr. Figure 5 plots $\varepsilon_n(\zeta)$ just before the exit foil, showing essentially no emittance growth from the injected value. When the same beam is propagated in 20 mtorr, the beam tapers more quickly, and ε_n rises during the pulse, reaching a maximum value of 1.1 rad-cm. The results are in approximate agreement with a simple analytical model which assumes free expansion at the beam head and an equilibrium pinch in the beam body.

IV. ENERGY VARIATION (DIFFERENTIAL FOCUSING) TAILORING CELL

Description of Method: This scheme involved deliberately introducing a 10-20% energy variation in the beam and passing it through a magnetic lens tuned to focus the highest energy portion in the beam body onto a scattering foil.[4] Lower energy portions are overfocused and expand before striking the foil. FRIEZR uses the thin lens approximation to model this approach.

Simulation results for differential focusing cell: Figure 6 plots the beam radius at the nominal focal point (30 cm) of a beam injected through a lens at an initial radius of 5 cm. The desired beam taper is attained, although the difference between $a_{1/2}$ and a_{rms} indicates an undesirable core-halo current density profile. The system must be tuned very accurately; a shift in the scattering foil position of only 3 cm in either direction alters the taper dramatically.

V. SUMMARY AND REFERENCES

All three conditioning techniques are capable of producing the desired radius taper although the multi-foil method may not be acceptable because of foil scattering. The IFR cell can in principle produce an excellent beam taper for stabilizing hose, but the differential focusing method is more compatible with the ATA fast corrector coil and can produce similar beam tailoring profiles if carefully tuned.

1. S. Slinker, et al., "Beam Stability and Range Extension Predictions for the ATA Multi-Pulse Experiment," these proceedings.
2. R. Adler, Part. Accel. 12, 39 (1982).
3. R. Fernsler, et al., "Foil Transport and Conditioning Cells," these proceedings.
4. W. Fawley, et al, "Conditioning Cell Design", these proceedings.
5. R. Hubbard, et al, Bull. Am. Phys. Soc. 32, 1718 (1987).

*Work supported by the Defense Advanced Research Projects Agency, ARPA Order No. 4395, Amendment 80, monitored by the Naval Surface Warfare Center.

Distribution List*

Naval Research Laboratory
4555 Overlook Avenue, S.W.

Attn: CAPT J. J. Donegan, Jr. - Code 1000
Dr. M. Lampe - Code 4792 (20 copies)
Dr. T. Coffey - Code 1001
Head, Office of Management & Admin - Code 1005
Deputy Head, Office of Management & Admin - Code 1005.1
Directives Staff, Office of Management & Admin - Code 1005.6
Director of Technical Services - Code 2000
ONR - Code 0124
NRL Historian - Code 2604
Dr. W. Ellis - Code 4000
Dr. J. Boris - Code 4040
Dr. M. Picone - Code 4040
Dr. E. Oran - Code 4040
Dr. M. Rosen - Code 4650
Dr. M. Haftel - Code 4665
Dr. S. Ossakow - Code 4700 (26 copies)
Dr. V. Patel - Code 4701
Dr. A. Robson - Code 4708
Dr. M. Friedman - Code 4732
Dr. R. Meger - Code 4750
Dr. J. Antoniades - Code 4751
Dr. T. Peyser - Code 4751
Dr. D. Murphy - Code 4751
Dr. R. Pechacek - Code 4750.1
Dr. G. Cooperstein - Code 4770
Dr. A. Ali - Code 4780
Dr. D. Colombant - Code 4790
Dr. R. Fernsler - Code 4790 (20 copies)
Dr. I. Haber - Code 4790
Dr. R. F. Hubbard - Code 4790 (20 copies)
Dr. G. Joyce - Code 4790 (20 copies)
Dr. Y. Lau - Code 4790
Dr. S. P. Slinker - Code 4790 (20 copies)
Dr. P. Sprangle - Code 4790
Dr. C. M. Tang - 4790
Dr. J. Krall - Code 4790
B. Pitcher - Code 4790A
Code 4790 (20 copies)
Dr. S. Gold - Code 4793
Dr. C. Kapetanakos - Code 4795
Mr. P. Boris - SAIC (Code 5166)
Library - Code 2628 (22 copies)
D. Wilbanks - Code 2634
Code 1220

* Every name listed on distribution gets one copy except for those where extra copies are noted.

Advanced Scientific Concepts, Inc.
2441 Foothill Lane
Santa Barbara, CA 93105
Attn: Dr. Roger Stettner

Advanced Technologies Research
14900 Sweitzer Lane
Laurel, MD 20707
Attn: Mr. Daniel Weldman

The Aerospace Corporation
Mail Stop M2-269
P. O. Box 92957
Los Angeles, CA 90009
Attn: Dr. David L. McKenzie
Dr. Carl J. Rice

AFATL/DLJW
Elgin Force Base, FL 32542
Attn: MAJ Louis W. Seller, Jr.

Air Force Office of Scientific Research
Physical and Geophysical Sciences
Bolling Air Force Base
Washington, DC 20332
Attn: Major Bruce Smith

Air Force Weapons Laboratory
Kirtland Air Force Base
Albuquerque, NM 87117-6008
Attn: Dr. William L. Baker (AFWL/NTYP)
Dr. Brendan B. Godfrey
Dr. Inara Kuck

Applied Physics Laboratory
The Johns Hopkins University
Asst. to Dir. for Tech. Assessment
Johns Hopkins Road
Laurel, MD 20707
Attn: Dr. Samuel Koslov

Armed Forces Radiobiology
Research Institute
Chief, MRAD
NMC-NCR
Bethesda, MD 20814-5145
Attn: LCDR J. P. Jacobus

U. S. Army Ballistics Research Laboratory
Aberdeen Proving Ground, Maryland 21005
Attn: Dr. Donald Eccleshall (DRXBR-BM)
Dr. Anand Prakash
Dr. Clinton Hollandsworth

Avco Everett Research Laboratory
2385 Revere Beach Pkwy
Everett, Massachusetts 02149
Attn: Dr. R. Patrick
Dr. Dennis Reilly

Ballena Systems Corporation
P. O. Box 752
Alameda, CA 94501
Attn: Dr. Adrian C. Smith
Dr. William E. Wright

Ballistic Missile Def. Ad. Tech. Ctr.
P.O. Box 1500
Huntsville, Alabama 35807
Attn: Dr. M. Hawie (BMDSATC-1)
Dr. M. J. Lavan (BMDATC-E)
Mr. Dan Whitener

The Boeing Aerospace Company
MS-2E30
Box 3999
Seattle, WA 98124
Attn: Dr. Robert C. Milnor

Booz, Allen, and Hamilton
Crystal Square 2, Suite 1100
1725 Jefferson Davis Highway
Arlington, VA 22202-4136
Attn: Dr. Charles M. Huddleston

Brobeck and Associates
1235 10th Street
Berkeley, CA 94710
Attn: Dr. Francis C. Younger

Chief of Naval Material
Office of Naval Technology
MAT-0712, Room 503
800 North Quincy Street
Arlington, VA 22217
Attn: Dr. Eli Zimet

Commander
Space and Naval Warfare Systems Comman
National Center 1, Room 8E08
Washington, DC 20363-5100
Attn: RADM Robert L. Topping

Cornell University
369 Upson Hall
Ithaca, NY 14853
Attn: Prof. David Hammer

Defense Advanced Research Projects Agency
1400 Wilson Blvd.
Arlington, VA 22209
Attn: Dr. H. L. Buchanan
Dr. B. Hui

Defense Nuclear Agency
Washington, DC 20305
Attn: Dr. Muhammad Owais (RAAE)
Dr. Michael Frankle
Dr. R. Gullickson

Department of Commerce
National Inst.of Standards and Tech.
Building 245, B-102
Washington, DC 20234
Attn: Dr. Mark A. D. Wilson
Dr. Steven M. Seltzer

Department of Energy
Washington, DC 20545
Attn: Dr. Wilmot Hess (ER20:GTN,
High Energy and Nuclear Physics)
Mr. Gerald J. Peters (G-256)

Department of the Navy
Chief of Naval Operations
The Pentagon
Washington,DC 20350
Attn: CAPT T. L. Sanders (OP981N3)
LCDR John Stanovich (OP981SDI)
LCDR Donald Melick (OP981SD)
Dr. Steve Bravy (OP981SDI)
Mr. Greg Montieth

Directed Technologies, Inc.
4001 Fairfax Drive, Suite 775
Arlington, VA 22203
Attn: Mr. Ira F. Kuhn
Dr. Nancy Chesser
Dr. Arthur Lee
Ms. Marla Shain

Directed Technologies, Inc.
5945 Pacific Center Blvd.
Suite 510
San Diego, CA 92121
Attn: Dr. Robert A. Jacobsen

Dr. Harald O. Dogliani
P. O. Box 503
Los Alamos, NM 87544

C. S. Draper Laboratories
555 Technology Square
Cambridge, Massachusetts 02139
Attn: Dr. E. Olsson

ESL, Inc.
Mail Stop M-4216
495 Java Drive
Sunnyvale, CA 94088
Attn: Dr. Robert A. Marth

FM Technologies, Inc.
10529B Braddock Road
Fairfax, VA 22032
Attn: Dr. F. M. Mako

GA Technologies, Inc.
P. O. Box 85608
Code 02/503
San Diego, CA 93138
Attn: Dr. Vincent Chen
Dr. Hiroyuki Ikez

General Dynamics Corporation
1745 Jefferson Davis Highway
Suite 1000
Arlington, VA 22202
Attn: Dr. Daniel W. Roth

General Dynamics Corporation
Pomona Division
1675 W. Mission Blvd.
P. O. Box 2507
Pomona, CA 92769-2507
Attn: Dr. Ken W. Hawko
Mr. C. L. Featherstone

Grumman Corporation
Grumman Aerospace Research Ctr.
Bethpage, NY 11714-3580
Attn: Dr. Richard G. Madonna

Headquarters, Department of Army
DAMOFDE, Room 2D547
The Pentagon
Washington, DC 20310-0460
Attn: LTCOL Lou Goldberg

HQ Foreign Technology Division
Wright-Patterson AFB, OH 45433
Attn: TUTD/Dr. C. Joseph Butler

HQ USAF/TXN
Patrick Air Force Base, FL 32925
Attn: CAPT Joseph Nicholas

Hudson Institute
Center for Naval Analyses
Alexandria, VA 22302
Attn: Dr. F. Bomse

Hy-Tech Research Corp.
P. O. Box 3422 FSS
Radford, VA 24143
Attn: Dr. Edward Yadlowsky

Idaho Engineering National Lab.
P. O. Box 1625
Idaho Falls, ID 83415
Attn: Dr. Francis Tsang

Institute for Defense Analyses
1801 N. Beauregard Street
Alexandria, VA 22311
Attn: Dr. Deborah Levin
Ms. M. Smith

IRT Corporation
3030 Callan Road
San Diego, CA 92121
Attn: Dr. David Phelps

JAYCOR
11011 Torreyana Road
P. O. Box 85154
San Diego, CA 92138-9259
Attn: Dr. Franklin S. Felber
Dr. Seung Kai Wong

JAYCOR
39650 Libery Street, Suite 320
Freemont, CA 94538
Attn: Dr. Kendal Casey

Joint Institute for Laboratory
Astrophysics
National Bureau of Standards and
University of Colorado
Boulder, CO 80309
Attn: Dr. Arthur V. Phelps

Kaman Sciences
P. O. Draver OO
Santa Barbara, CA 93102
Attn: Dr. W. Hobbs

La Jolla Institute
P. O. Box 1434
La Jolla, CA 92038
Attn: Dr. K. Brueckner

Lawrence Berkeley Laboratory
University of California
Berkeley, CA 94720
Attn: Dr. Edvard P. Lee
Dr. Thomas Fessenden
Dr. William Fawley
Dr. Roger Bangerter

Lawrence Livermore National Laboratory
University of California
Livermore, California 94550
Attn: Mr. Arthur G. Cole
Dr. Michael Delong
MAJ Kenneth Dreyer
Dr. Ed Farley
Dr. Alex Glass
Dr. George Craig
Dr. C. V. Johnson, III
Dr. George Kamin
Dr. V. Kelvin Neil
Dr. Arthur C. Paul
Mr. Louis Reginato
Mr. Doyle Rogers
Dr. Dennis R. Slaughter
Dr. David Whittum
Dr. Simon S. Yu
Dr. Frank Chambers
Dr. James W.-K. Mark, L-477
Dr. William Barletta
Dr. William Sharp
Dr. John K. Boyd
Dr. John Clark
Dr. George J. Caporaso
Dr. Donald Prosnitz
Dr. John Stevart
Dr. Y. P. Chong
Dr. Hans Kruger
Dr. Thaddeus J. Orzechovski
Dr. John T. Weir
Dr. Yu-Jiuan Chen

Dr. James E. Leiss
13013 Chestnut Oak Drive
Gaithersburg, MD 20878

Lockheed Missiles and Space Co.
3251 Hanover St.
Bldg. 205, Dept 92-20
Palo Alto, CA 94304
Attn: Dr. John Siambis

Los Alamos National Laboratory
P.O. Box 1663
Los Alamos, NM 87545
Attn: Dr. L. Thode
Dr. H. Dogliani, MS-5000
Mr. R. Carlson, MS-P940
Dr. Carl Ekdahl, MS-D410
Dr. Joseph Mack
Dr. Melvin I. Buchwald
Dr. David C. Moir
Dr. Daniel S. Prono
Dr. S. Czuchlevski
Dr. Thomas P. Starke
Dr. Donald D. Cobb, D466
Dr. Robert R. Karl, D466
Dr. William B. Maier
Dr. John P. Rink
Dr. David Chamberlin

Maxwell Laboratories Inc.
8888 Balboa Avenue
San Diego, CA 92123
Attn: Dr. Ken Whitham
Dr. S. Echouse

McDonnell Douglas Research Laboratories
Dept. 223, Bldg. 33, Level 45
Box 516
St. Louis, MO 63166
Attn: Dr. Carl Leader
Dr. Frank Bieniosek
Dr. John Honig

Mission Research Corporation
1720 Randolph Road, S.E.
Albuquerque, NM 87106
Attn: Dr. Thomas Hughes
Dr. Lawrence Wright
Dr. Kenneth Struve
Dr. Michael Mostrom
Dr. Dale Welch

Mission Research Corporation
P. O. Drawer 719
Santa Barbara, California 93102
Attn: Dr. C. Longmire
Dr. N. Carron

Mission Research Corporation
8560 Cinderbed Road
Suite 700
Newington, VA 22122
Attn: Dr. Khanh Nguyen

National Inst. of Standards & Tech.
Gaithersburg, Maryland 20760
Attn: Dr. Mark Wilson

National Inst. of Standards & Tech.
Radiation Physics Bldg. Room C229
Washington, DC 20234
Attn: Dr. Wayne Cassatt

National Security Agency
4928 College Avenue
College Park, MD 20740
Attn: Dr. Albert J. Leyendecker

Naval Ocean Systems Center
San Diego, CA 92152
Attn: CAPT James Fontana
Mrs. Teresita Finch
Dr. Rodney Buntzen

Naval Postgraduate School
Physics Department (Code 61)
Monterey, CA 93940
Attn: Prof. John R. Neighbours
Prof. Fred Buskirk
Prof. Kai Woehler
Prof. Xavier Maruyama

Naval Surface Warfare Center
Dahlgren, VA 22448-5000
Attn: Dr. E. M. Williams
Mr. C. E. Gallaher
Mr. Lawrence Luessen
Ms. Theresa Houghton
Dr. Ronald J. Gripshover
Dr. S. L. Moran
Dr. Edwin Ball

Naval Surface Warfare Center
White Oak Laboratory
Code R-41
Silver Spring, Maryland 20903-5000
Attn: CAPT R. P. Fuscaldo
Dr. Thomas A. Clare
CAPT R. W. Moore
Dr. Ira Blatstein
Mr. Kenneth Caudle
Mr. Carl Larson
Dr. Robert DeWitt
Dr. Ralph Schneider
Dr. Joel Miller
Dr. Stanley Stern
Dr. Omer Goktepe
Dr. A. L. Licht
Dr. Joon Choe
Mr. David Demske
Dr. Jag Sharma
Mr. W. M. Hinckley
Dr. H. S. Uhm
Dr. R. Fiorito
Dr. R. Stark
Dr. H. C. Chen
Dr. D. Rule
Dr. Matt Brown
Mrs. Carolyn Fisher (G42)
Dr. Eugene E. Nolting (H23)

Naval Technical Intelligence Center
Code DA52
4301 Suitland Road
Washington, DC 20395
Attn: Mr. Mark Chapman

New Mexico State University
Research Center
Box RC
Las Cruces, NM 88003-0001
Attn: Dr. Leon J. Radziemski

Northeastern University
Dept. of Elec. Engineering
360 Huntington Avenue
Boston, MA 02115
Attn: Dr. Philip Serafim

North Star Research Corp.
5555 Zuni, S. E.
Albuquerque, NM 87104
Attn: Dr. Richard Adler

Oak Ridge National Laboratory
Health & Safety Research Div.
P. O. Box X
Oak Ridge, TN 37830
Attn: Dr. Rufus H. Ritchie
Dr. O. Crawford

Office of the Chief of Naval Operation
Strategic and Theatre Nuclear Warfare
OP-654E4
The Pentagon
Washington, DC 20350
Attn: Dr. Yong S. Park

Office of Naval Research
800 North Quincy Street
Arlington, VA 22217
Attn: Dr. C. W. Roberson
Dr. F. Saalfeld

Office of Naval Research (2 copies)
Department of the Navy
Code 01231C
Arlington, VA 22217

Office of Under Secretary of Defense
Research and Engineering
Room 3E1034
The Pentagon
Washington, DC 20301
Attn: Dr. John MacCallum

OSWR
P. O. Box 1925
Washington, DC 20013
Attn: Dr. Jose F. Pina

PhotoMetrics, Inc.
4 Arrow Drive
Woburn, MA 01801
Attn: Dr. Irving Kofsky

Physics International, Inc.
2700 Merced Street
San Leandro, CA. 94577
Attn: Dr. E. Goldman
Dr. James Benford
Dr. George B. Frazier
Mr. Ralph Genuario

Princeton University
Plasma Physics Laboratory
Princeton, NJ 08540
Attn: Dr. Francis Perkins, Jr.

Pulse Sciences, Inc.
600 McCormack Street
San Leandro, CA 94577
Attn: Dr. Sidney Putnam
Dr. Vernon Bailey
Dr. M. Tiefenbach
Dr. J. Edighoffer
Mr. James Fockler

Pulse Sciences, Inc.
2001 Wilshire Boulevard
Suite 600
Santa Monica, CA 90403
Attn: Dr. John R. Bayless

R&D Associates
301A South West Street
Alexandria, VA 22314
Attn: Mr. Ihor Vitkovitsky
Dr. Peter Turchi

The Rand Corporation
2100 M Street, NW
Washington, DC 20037
Attn: Dr. Nikita Wells
Mr. Simon Kassel

Sandia National Laboratory
Albuquerque, NM 87115
Attn: Dr. Collins Clark
Dr. John Freeman/1241
Dr. Charles Frost
Dr. Gerald N. Hays
Dr. Michael G. Mazarakis/1272
Dr. John Wagner/1241
Dr. Ron Lipinski/1274
Dr. James Poukey
Dr. Milton J. Clauser/1261
Dr. Kenneth R. Prestwich/1240
Dr. Kevin O'Brien
Dr. Isaac R. Shokair
Dr. J. Pace VanDevender/1200
Dr. J. T. Crow
Dr. S. Shope
Dr. B. N. Turman
Dr. C. Olson
Dr. Richard Adams
Dr. Malcolm Buttram
Mr. Charles Crist
Dr. Susan Fisher
Dr. John Keizur
Dr. Gordon T. Leifeste
Dr. Raymond W. Lemke
Dr. Juan Ramirez
Dr. James Rice
Dr. Michael Wilson

Science Applications Intl. Corp.
2109 Air Park Road, S. E.
Albuquerque, NM 87106
Attn: Dr. R. Richardson
Dr. Michael D. Haworth
Dr. Alan J. Toepfer

Science Applications Intl. Corp.
5150 El Camino Road
Los Altos, CA 94022
Attn: Dr. R. R. Johnston
Dr. Leon Feinstein
Dr. Douglas Keeley
Dr. E. Roland Parkinson

Science Applications Intl. Corp.
1710 Goodridge Drive
McLean, VA 22102
Attn: Mr. W. Chadsey
Dr. A Drobot
Dr. K. Papadopoulos
Dr. William W. Rienstra
Dr. Alfred Mondelli
Dr. D. Chernin
Dr. R. Tsang
Dr. J. Petillo
Dr. G. Bourianoff
Ms. K. Wilson

Science Research Laboratory, Inc.
1600 Wilson Boulevard
Suite 1200
Arlington, VA 22209
Attn: Dr. Joseph Mangano
Dr. Daniel Birx

Commander
Space & Naval Warfare Systems Command
PMW-145
Washington, DC 20363-5100
Attn: CDR W. Fritchie
Mr. D. Merritt

Space Power Institute
315 Leach Science Center
Auburn University
Auburn, AL 36845-3501
Attn: Prof. M. Frank Rose

Spectra Technology
2755 Northup Way
Bellevue, WA 98004
Attn: Dr. Dennis Lowenthal
Dr. Steve Baughoum
Dr. James Ewing

SRI International
PS0-15
Molecular Physics Laboratory
333 Ravenswood Avenue
Menlo Park, CA 94025
Attn: Dr. Donald Eckstrom
Dr. Kenneth R. Stalder
Dr. Roberta Saxon
Dr. Jay Dickerson

Strategic Defense Initiative Org.
SDIO/T/DEO
The Pentagon
Washington, DC 20301-7100
Attn: *COL Thomas Meyer (DEWO)*
LTC Michael toole (DEWO)
MAJ J. Wills
Dr. Dwight Duston
LTC Ed Pogue
Dr. Kevin Probst
Dr. Charles Sharn

System Planning Corporation
1500 Wilson Boulevard, Room 1213W
Arlington, VA 22209
Attn: Mr. James T. Lacatski

Titan/Spectron, Inc.
P. O. Box 4399
Albuquerque, NM 87196
Attn: Dr. R. Bruce Miller
Dr. John Smith

Titan Systems, Inc.
5910 Pacific Center Blvd.
San Diego, CA 92121
Attn: Dr. R. M. Dove, Jr.

Tetra Corporation
4905 Hawkins Street, N. E.
Albuquerque, NM 87109-4345
Attn: Mr. William Money

University of California
Physics Department
Irvine, CA 92664
Attn: Dr. Gregory Benford
Dr. Norman Rostoker

University of California
San Diego, CA 92110
Attn: Dr. Marshall N. Rosenbluth

UCLA
Physics Department
Los Angeles, CA 90024
Attn: Dr. F. Chen
Dr. C. Joshi
Dr. J. Dawson
Dr. N. Luhmann
Dr. W. Barletta
Dr. T. Katsouleas

University of Colorado
Dept. of Astrophysical, Planetary
& Atmospheric Sciences
Boulder, CO 80309
Attn: Dr. Scott Robertson

University of Illinois at Chicago
Dept. of Physics
P. O. Box 4348
Chicago, IL 60680
Attn: Dr. Charles K. Rhodes

University of Maryland
College Park, MD 20742
Attn: Dr. J. Goldhar
Dr. W. Destler
Dr. C. Striffler
Dr.Moon-Jhong Rhee

University of Michigan
Dept. of Nuclear Engineering
Ann Arbor, MI 48109
Attn: Prof. Terry Kammash
Prof. R. Gilgenbach

University of New Mexico
Dept. of Chem. & Nuclear Engineering
Albuquerque, NM 87131
Attn: Prof. Stanley Humphries

Commander
U. S. Army Laboratory Command
2800 Powder Mill Road
Adelphi, MD 20783-1145
Attn: George Albrecht (AMSLC-TP-PL)

U. S. Army Combined Army Center
ATZL-CAG
Ft. Leavenworth, KS 68027-5000
Attn: LTC Orville Stokes

Yale University
Mason Laboratory
New Haven, CN 06520
Attn: Dr. Ira Bernstein

Director of Research
U.S. Naval Academy
Annapolis, MD 21402 (2 copies)